No Evidence of Gas-Liquid Coexistence in Dipolar Hard Spheres

Lorenzo Rovigatti and John Russo
Dipartimento di Fisica, Università di Roma La Sapienza, Piazzale Aldo Moro 5, 00185 Roma, Italy

Francesco Sciortino
Dipartimento di Fisica and CNR-ISC, Università di Roma La Sapienza, Piazzale Aldo Moro 5, 00185 Roma, Italy
(Received 1 August 2011; published 28 November 2011)

We report accurate calculations of the particle density of states in the dipolar hard-sphere fluid. Implementing efficient and tailored Monte Carlo algorithms, we are able to explore, in equilibrium, the low temperature region where a phase separation between a dilute gas of chain ends and a high-density liquid of chain junctions has been predicted to occur. Our data clearly show that the density of states remains always single peaked, definitively excluding the possibility of critical phenomena in the investigated temperature and density region. The analysis of the low temperature configurations shows that at low densities particles preferentially self-assemble into closed rings, strongly suppressing the chain ends concentration.

DOI: 10.1103/PhysRevLett.107.237801 PACS numbers: 61.20.Ja, 61.25.Em, 75.50.Mm

The dipolar hard-sphere (DHS) model is a paradigm for the self-assembly of anisotropic particles [1] and a challenge for present day theories of fluids. For these reasons, significant effort has been put into the direction of establishing its phase diagram. Despite the simplicity of the model (a point dipole at the center of a hard sphere) contrasting opinions exist about its putative gas-liquid critical point and on the location of the associated first-order phase transition. The pioneering work of de Gennes and Pincus [2] pointed out that, in the dilute limit, DHS particles experience an effective isotropic attraction. This effective attraction, being the magnetic analogue of the molecular van der Waals (vdW) force, should promote at low temperature T a liquid-gas phase separation as in ordinary vdW fluids. It was soon realized that the highly anisotropic character of the dipole-dipole interaction, which promotes the self-assembly of the dipoles into chains, could impose a local order significantly different from the one characteristic of vdW fluids, perhaps completely suppressing the isotropic phase coexistence [3–5]. Indeed the first computer simulation studies, although plagued by equilibration issues, provided evidence of an extended nose-to-tail chaining and found contradictory evidence of a phase transition [6–8].

The debate on the existence of a critical point in DHS was rejuvenated by additional simulations studies [9–11] and by a seminal paper by Tlusty and Safran (TS) [12]. A new type of phase transition was postulated, sustained, rather than suppressed, by the self-assembly of the dipoles. The transition is hierarchical and involves a subtle competition between chain ends and chain junctions, leading to two coexisting phases with different topology: a ''gas'' of chains and a networklike ''liquid'' rich in junctions. The possibility of such a phase transition, which depends crucially on the number density of topological defects (chain ends and junctions) and their scaling with density, results in a peculiar reentrant phase diagram, in which the density ρ of the liquid phase approaches the vanishing ρ of the gas phase on cooling. Such a peculiar phase diagram has been recently observed in models of asymmetric patchy particles [13,14]. A close mapping between patchy particle models and DHS has been recently attempted [15]. A recent thermodynamic perturbation theory [16], in which chain association is explicitly accounted for, suggests instead the existence of a standard gas-liquid coexistence.

The long relaxation time of the self-assembled structures and the intrinsic slowness of the long range dipolar calculations have prevented accurate studies of the DHS low T behavior. Ingenious numerical studies have evaluated the critical point of sequences of models which asymptotically tend to DHS [17–20]. Based on extrapolation of DHS plus an attractive isotropic Yukawa component [17], binary mixtures of apolar and dipolar hard spheres [19] or charged dumbbells [18,20] the location of the putative gas-liquid critical point has been restricted to the window $\rho \lesssim 0.1$ and $T < 0.16$.

In this Letter we use highly efficient simulation techniques and extended computational resources to address the question of whether a gas-liquid phase transition exists in DHS. These techniques allow us to access in equilibrium the T region where theories and previous numerical attempts had predicted a gas-liquid coexistence. We definitively prove that no sign of critical behavior is observed. The analysis of the low T data reveals the presence of extended rings of nose-to-tail particles which deplete the concentration of chain ends.

The pair interaction potential between two dipolar hard spheres i and j is

$$u(i,j) = u_{\mathrm{HS}}(r_{ij}) + \frac{\boldsymbol{\mu}_i \cdot \boldsymbol{\mu}_j - 3(\boldsymbol{\mu}_i \cdot \hat{\mathbf{r}}_{ij})(\boldsymbol{\mu}_j \cdot \hat{\mathbf{r}}_{ij})}{r_{ij}^3}, \quad (1)$$

where $\mathbf{r}_{ij}$ is the vector connecting the centers of particle i and j, $u_{\mathrm{HS}}(r_{ij})$ is the hard-sphere potential, and $\boldsymbol{\mu}_i$ is the dipole moment of particle i. In the following, the Boltzmann constant $k_B = 1$, $\beta = 1/T$, lengths are measured in units of the particles diameter σ and energy in units of μ^2/σ^3. In these units, the DHS pair potential has an absolute minimum $u = -2$ in the nose-to-tail contact geometry and a relative minimum $u = -1$ in the side-to-side antiparallel geometry. The difficulty in simulating this model arises from the long range nature of the dipolar interaction and by the low T. To provide an idea of the computational effort requested, consider that the Metropolis acceptance probability of extracting a particle belonging to an infinite linear chain at the lowest studied T is less than 10^{-12}. To speed up the calculations we introduce special Monte Carlo (MC) moves specifically designed for DHS, or adapted from state-of-art techniques. To sample the conformations of the self-assembled structures we implement a version of the aggregation-volume-bias (AVB) algorithm [21], in which we define two virtual bonding regions (BR) on the poles of the particles, shaped as truncated cones. We then encode special moves in which a particle located inside the BR of a randomly selected particle moves out of the BR or a particle outside the BR moves into the BR, accepting the move with the proper acceptance probability. To speed up the insertion and removal of particles from the system we adopt the technique introduced by Caillol [9] [and adapted for grand canonical MC (GCMC) by Ganzenmüller *et al.* [17]] which takes into account the value of the local electric field to bias GCMC moves. Finally, to uniformly sample the particle density of states (despite the large free energy difference between low and high-density phases at fixed activity), and to effectively parallelize our simulations, we perform successive umbrella sampling (SUS) simulations [22]. With this method, the region to be explored is partitioned in overlapping windows of ΔN particles. Each region is sampled with GCMC simulations with appropriate boundary conditions [23], providing a speed up proportional to the number of windows explored in parallel (200 in our case). The SUS method allows us to obtain the distribution of density fluctuations $P(\rho)$ at fixed activity $z = e^{\beta\mu}$ (where μ is the chemical potential). We then evaluate $P(\rho)$ at different z and nearby T by means of histogram reweighting techniques [24]. We investigate a system of up to $N = 1000$ particles in a box size of $L = 19.26$ via windows, overlapping by one particle, of width $\Delta N = 6$. This corresponds to the density region $\rho \in [0, 0.14]$. We have investigated three different T, namely $T = 0.125$, 0.140, and 0.150, all below the lowest estimate $T = 0.153$ at which the critical point is predicted to exist [11,16,17,19,20]. Long range dipolar interactions are taken into account using Ewald sums with conducting boundary conditions [25]. We have also carried out complementary NVT simulations for a system of $N = 5000$ particles at four equispaced T (from $T = 0.125$ to $T = 0.170$) for six different ρ, ranging from $\rho = 0.007$ to $\rho = 0.140$. In the GCMC simulations, the frequency of insertions (or deletions), AVB moves, and regular rotations (or translations) is, respectively, 1:50:50. In the NVT ensemble simulations the frequency between AVB moves and rotations (or translations) is 50:50.

In order to investigate the local connectivity and be able to classify particles into specific local geometries a criterion to define a bond between two particles is needed. Criteria found in the literature are based on cutoff distances [17,26] or pair interaction energy thresholds [6,17,27,28]. We combine these criteria by considering particles i and j to be bonded if $r_{ij} < r_b$ and $u(i, j) < 0$, where r_b is the position of the first minimum of the $g(r)$. Because the position of the minimum is found to be only slightly dependent on T and ρ, we choose $r_b = 1.3$ throughout this work. We use this bonding criterion to compute cluster size distributions, to partition clusters into chains, rings, and branched structures as well as to evaluate the concentration of chain ends and junctions. We also use it to evaluate the bond-bond autocorrelation function to verify that the length of the NVT simulations is large enough for the bonding pattern to completely lose memory of its original state.

Figure 1 shows the main result of this Letter, $P(\rho)$ for several values of z and T. On decreasing T, the noise level increases, signaling the difficulty of properly sampling configuration space, despite the length of the simulation (extending to ten months of computation for each of the 200 Xeon 5550 CPU cores). For all T, the shape of $P(\rho)$ excludes the presence of a gas-liquid coexistence down to $T = 0.125$. Two minor peaks are also found, both located at very low densities. A peak at $N \sim 10$–15 (corresponding to $\rho \sim 0.0015$–0.002) is observed at all T. One further peak around $N \approx 20$–25 appears at $T = 0.14$ and becomes prominent at the lowest T, as shown in the inset of Fig. 1(c). To identify the nature of these two peaks we perform a finite size study of the low density region, confirming that the first peak is always located at $N \sim 10$–15, while the position in N of the second peak scales linearly with the box size. The presence of constant N peaks is typically associated with self-assembly processes of aggregates with a preferential size, which does not depend on the system volume [29,30]. The second peak reflects the presence of linear chains which percolate via boundary conditions. Compared to chains of the same size, they are energetically stabilized by the presence of one additional bond.

To clarify the origin of the self-assembly peak we investigate in detail the structure of the fluid at low T, analyzing NVT configurations. The number of particles employed ($N = 5000$) and the large box sizes, beside improving the quality of the data, suppress any finite size effects associated with percolating chains. Based on the

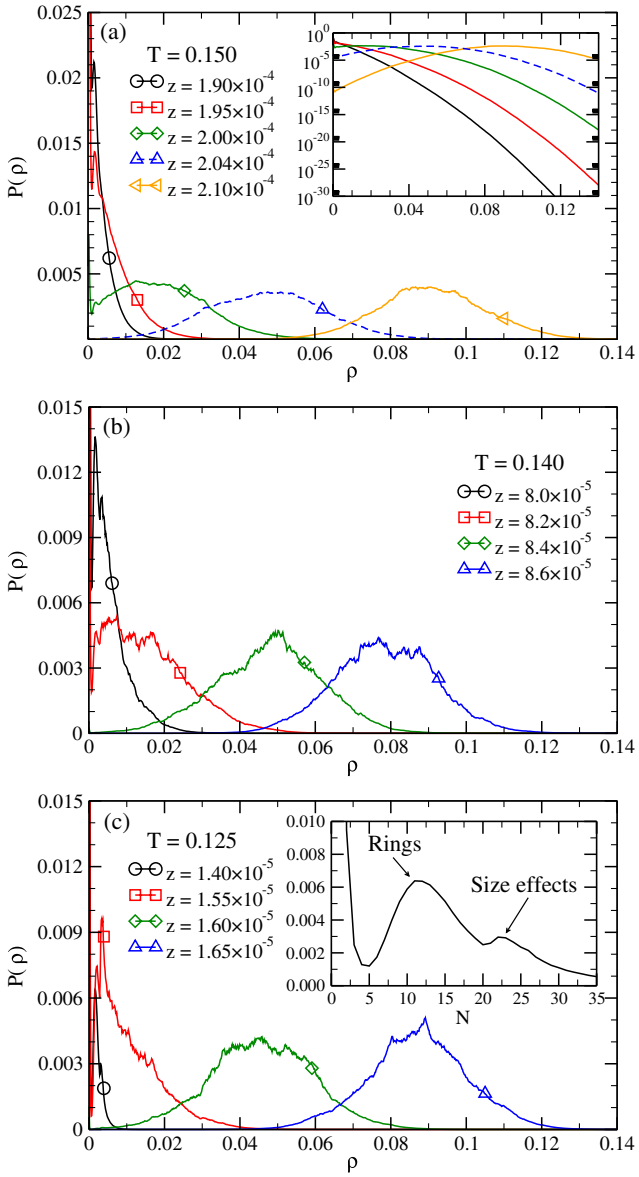

FIG. 1 (color online). Distribution of density fluctuations $P(\rho)$ for different activities z at (a) $T = 0.150$, (b) $T = 0.140$, and (c) $T = 0.125$. Curves are obtained via histogram reweighting in z, starting from the value of z at which the simulations were performed: (a) $z = 2.04 \times 10^{-4}$ (dashed line), (b) $z = 9.00 \times 10^{-5}$, and (c) $z = 1.535 \times 10^{-5}$. Symbols are added on each curve in order to increase black and white readability. Inset: (a) lin-log representation of $P(\rho)$. (c) $P(N)$ for $z = 1.4 \times 10^{-5}$ in the range $N \in [0, 35]$.

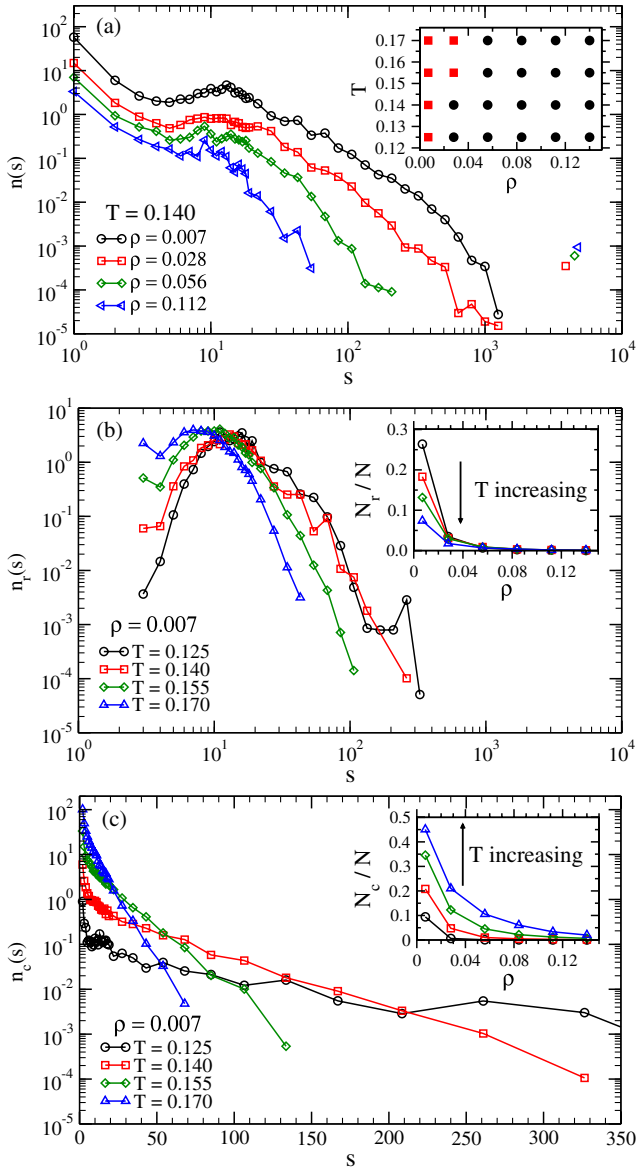

FIG. 2 (color online). (a) Number of clusters $n(s)$ of size s at $T = 0.140$ and different ρ in a system of $N = 5000$ particles [$\sum_s sn(s) = N$]. Clusters with $s > 3000$ (disconnected points) are percolating. The inset shows the percolating (black circle) and nonpercolating (red squares) state points. Number of rings $n_r(s)$ (b) and of chains $n_c(s)$ (c) of size s at $\rho = 0.007$ and different T. The inset shows the fraction of particles in rings N_r/N (b) and in chains N_c/N (c) as a function of ρ. Note the inverted order with T of N_c/N and N_r/N as well as the exponential tail only for large s in $n_c(s)$. Lines are guides for the eye.

bonding criterion adopted, we partition particles into chains, rings, or branched clusters [6,17,26,28], according to their topology. We find that clusters with $s \lesssim 40$ are mostly rings or chains, i.e., only a few junctions are present in small clusters. Beyond a certain ρ, the system is always percolating, that is, more than 50% of its equilibrium configurations contains a spanning (infinite) cluster. The percolation ρ becomes as small as $\rho \approx 0.01$ when $T = 0.125$, as shown in the inset of Fig. 2(a). The ρ dependence of the cluster size distribution $n(s)$ is shown in Fig. 2(a). A peak at $N \approx 10$–15, i.e., at the same location as the one observed in $P(\rho)$, is present at all T, confirming that such a peak arises from the preferential self-assembly of the particles in particular clusters. Separating $n(s)$ in its ring [$n_r(s)$, Fig. 2(b)], chain [$n_c(s)$, Fig. 2(c)], and

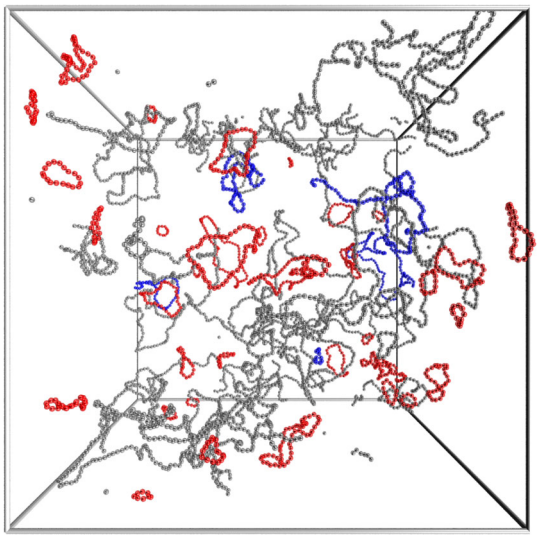

FIG. 3 (color online). Snapshot of a typical equilibrium configuration with $N = 5000$ particles at $T = 0.125$ and $\rho = 0.007$. Rings are coded in red, chains are coded in blue, while all the other clusters are depicted in gray.

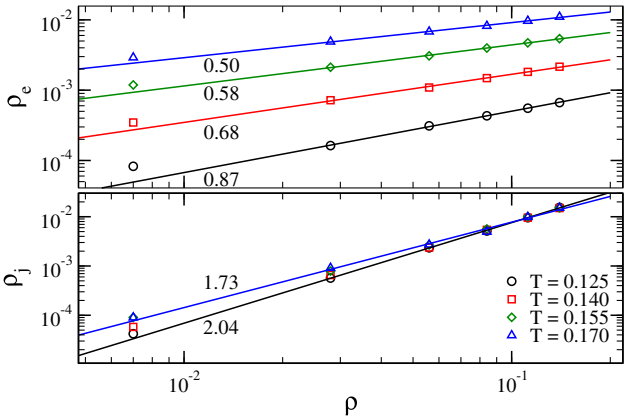

FIG. 4 (color online). Density of ends ρ_e and of junctions ρ_j as a function of ρ at all the studied T. Lines are power-law fits restricted to $\rho > 0.007$. The value of the best-fit exponent is indicated beside the lines. A significant T dependence is observed. Note that a drastic change in the bonding distance criterion results only in a slight change in the value of the junction exponent and in a 20% change in the end exponent, but both exponents retain their T dependence.

branched components, allows us to identify the rings as the structures responsible for the peak. Indeed, $n_r(s)$ is nonmonotonic, shows a tail which becomes progressively extended on cooling and is peaked at $N \approx 10$–15. $n_c(s)$ is monotonic, and decays exponentially only for large s, suggesting that the free energy cost of adding a particle to a chain becomes independent of the chain length only for $s \gtrsim 20$. The slope of the exponential tail decreases on cooling, signaling the progressive increase of the average chain length [6,28].

At the lowest T rings of size $10 \lesssim s \lesssim 100$ become more probable than chains of the same size and the total number of particles in rings N_r [inset of Fig. 2(b)] becomes larger than the number of particles in chains N_c [inset of Fig. 2(c)]. Such an increase in N_r on lowering T and ρ offers a possible hint on why the critical phenomenon is not observed. Indeed, rings are characterized by a small net total dipole moment, resulting in a small effective ring-ring interaction. The low density DHS thus progressively turn into a fluid of weakly interacting aggregates, providing an example of phase separation suppressed by self-assembly [31,32]. A snapshot of the $\rho = 0.007$ system is shown in Fig. 3.

Finally, we examine the ρ dependence of the concentration of chain ends ρ_e (particles with just one bonded neighbor) and of junctions ρ_j (particles with three bonded neighbors). In the mean-field TS theory both ρ_e and ρ_j follow a power law in ρ with exponents $1/2$ and $3/2$, respectively. These exponents play a major role, controlling the ρ dependence of the system free energy. Figure 4 shows ρ_e and ρ_j for all the studied state points. Only for $\rho > 0.007$, do ρ_e and ρ_j follow a power law, but with a T-dependent exponent. Moreover, the exponents appear to approach the values assumed in the TS theory only at the highest T studied. This strongly suggests that the competition between topological defects is not a viable mechanism for sustaining a critical point in DHS.

In conclusion, using powerful computational techniques, we have shown that the DHS system does not exhibit any sign of gas-liquid criticality in the window $0.125 < T < 0.150$ and $0 < \rho < 0.14$, i.e., even well below the region where such critical point was predicted to be located. We have also shown that at low T and low ρ there is an explosion of rings which appear to become the dominant topological clusters. We speculate that the absence of gas-liquid criticality is related to the fact that the low ρ nonpercolating fluid, being very rich in rings, is in a state in which all particles are close to their ground state energy and which has a larger translational entropy compared to the percolating phase.

We acknowledge support from ERC-226207-PATCHYCOLLOIDS and ITN-234810-COMPLOIDS. We thank P. J. Camp, S. Kumar, F. Romano, J. M. Tavares, P. I. C. Teixeira, and M. M. Telo da Gama for relevant discussions.

[1] J. Dudowicz, K. F. Freed, and J. F. Douglas, J. Chem. Phys. **111**, 7116 (1999).
[2] P. G. de Gennes and P. A. Pincus, Phys. Kondens. Mater. **11**, 189 (1970).
[3] R. van Roij, Phys. Rev. Lett. **76**, 3348 (1996).
[4] R. P. Sear, Phys. Rev. Lett. **76**, 2310 (1996).
[5] P. I. C. Teixeira, J. M. Tavares, and M. M. Telo da Gama, J. Phys. Condens. Matter **12**, R411 (2000).
[6] J. J. Weis and D. Levesque, Phys. Rev. Lett. **71**, 2729 (1993).

[7] M. E. van Leeuwen and B. Smit, Phys. Rev. Lett. **71**, 3991 (1993).
[8] K.-C. Ng, J. P. Valleau, G. M. Torrie, and G. N. Patey, Mol. Phys. **38**, 781 (1979).
[9] J.-M. Caillol, J. Chem. Phys. **98**, 9835 (1993).
[10] P. J. Camp, J. C. Shelley, and G. N. Patey, Phys. Rev. Lett. **84**, 115 (2000).
[11] R. Jia, H. Braun, and R. Hentschke, Phys. Rev. E **82**, 062501 (2010).
[12] T. Tlusty and S. A. Safran, Science **290**, 1328 (2000).
[13] J. Russo, J. M. Tavares, P. I. C. Teixeira, M. M. Telo da Gama, and F. Sciortino, Phys. Rev. Lett. **106**, 085703 (2011).
[14] J. Russo, J. Tavares, P. Teixeira, M. da Gama, and F. Sciortino, J. Chem. Phys. **135**, 034501 (2011).
[15] J. Tavares and P. Teixeira, Mol. Phys. **109**, 1077 (2011).
[16] Y. V. Kalyuzhnyi, I. A. Protsykevytch, and P. T. Cummings, Europhys. Lett. **80**, 56002 (2007).
[17] G. Ganzenmüller, G. N. Patey, and P. J. Camp, Mol. Phys. **107**, 403 (2009).
[18] J. C. Shelley, G. N. Patey, D. Levesque, and J. J. Weis, Phys. Rev. E **59**, 3065 (1999).
[19] N. G. Almarza, E. Lomba, C. Martín, and A. Gallardo, J. Chem. Phys. **129**, 234504 (2008).
[20] G. Ganzenmüller and P. J. Camp, J. Chem. Phys. **126**, 191104 (2007).
[21] B. Chen and J. I. Siepmann, J. Phys. Chem. B **105**, 11 275 (2001).
[22] P. Virnau and M. Müller, J. Chem. Phys. **120**, 10 925 (2004).
[23] B. J. Schulz, K. Binder, M. Müller, and D. P. Landau, Phys. Rev. E **67**, 067102 (2003).
[24] A. M. Ferrenberg and R. H. Swendsen, Phys. Rev. Lett. **61**, 2635 (1988).
[25] B. Smit and D. Frenkel, *Understanding Molecular Simulations* (Academic, New York, 1996).
[26] J. M. Tavares, J. J. Weis, and M. M. Telo da Gama, Phys. Rev. E **65**, 061201 (2002).
[27] D. Levesque and J. J. Weis, Phys. Rev. E **49**, 5131 (1994).
[28] J. M. Tavares, J. J. Weis, and M. M. Telo da Gama, Phys. Rev. E **59**, 4388 (1999).
[29] M. A. Floriano, E. Caponetti, and A. Z. Panagiotopoulos, Langmuir **15**, 3143 (1999).
[30] F. Lo Verso, A. Z. Panagiotopoulos, and C. N. Likos, Phys. Rev. E **79**, 010401 (2009).
[31] F. Sciortino, A. Giacometti, and G. Pastore, Phys. Rev. Lett. **103**, 237801 (2009).
[32] A. Reinhardt, A. J. Williamson, J. P. K. Doye, J. Carrete, L. M. Varela, and A. A. Louis, J. Chem. Phys. **134**, 104905 (2011).